Acta Cryst E CRYSTALLOGRAPHIC COMMUNICATIONS
ISSN 2056-9890

Crystal structure, Hirshfeld surface analysis and DFT calculations of 7-bromo-2,3-dihydropyrrolo-[2,1-*b*]quinazolin-9(1*H*)-one

Akmaljon Tojiboev,[a,b]* Burkhon Elmuradov,[c] Nuritdin Kattaev,[b] Asqar Abdurazakov,[c] Azizbek Nasrullayev[d] and Bakhodir Tashkhodjaev[c]

[a]University of Geological Sciences, Olimlar street, 64, Mirzo Ulugbek district, Tashkent, Uzbekistan, [b]Department of Chemistry, National University of Uzbekistan named after Mirzo Ulugbek, Tashkent, Uzbekistan, [c]S. Yunusov Institute of Chemistry of Plant Substances, Academy of Sciences of Uzbekistan, Tashkent, Uzbekistan, and [d]Department of Organic Synthesis and Bioorganic Chemistry, Samarkand State University, Samarkand, Uzbekistan. *Correspondence e-mail: a_tojiboev@yahoo.com

Received 13 July 2022
Accepted 2 August 2022

Edited by M. Weil, Vienna University of Technology, Austria

Keywords: crystal structure; 7-bromo-2,3-dihydropyrrolo[2,1-*b*]quinazolin-9(1*H*)-one; Hirshfeld surface analysis; DFT.

CCDC reference: 2194365

Supporting information: this article has supporting information at journals.iucr.org/e

The molecular structure of the title compound, $C_{11}H_9BrN_2O$, is almost planar. The benzene and pyrimidine rings are essentially coplanar, with r.m.s. deviations of 0.0130 Å, and the largest displacement is for the flap atom of the dihydropyrrole moiety [0.154 (7) Å]. Hirshfeld surface analyses revealed that the crystal packing is dominated by H···H, Br···H/H···Br and O···H/H···O interactions, and Br···Br interactions in the crystal structure are also observed. Theoretical calculations using density functional theory (DFT) with the B3LYP functional basis set gave numerical parameters for the frontier molecular orbitals.

1. Chemical context

Quinazolines are of significant interest for their various biological properties (Rajput *et al.*, 2012; Ramesh *et al.*, 2012; Khan *et al.*, 2014; Ajani *et al.*, 2016). This class of compounds is considered as an attractive target for medicinal chemists, because quinazoline and its derivatives are the scaffold of several potent antitumor drugs, for example the well-known *erlotinib* and *gefitinib* (Sordella *et al.*, 2004; Raymond *et al.*, 2000). Besides these two drugs, the Food and Drug Administration (FDA) has approved some other quinazolines as effective anticancer drugs, *viz*. *lapatinib* and *vandetanib*. In general, the reported biological activities of quinazolines include antibacterial, anti-inflammatory, CNS depressant, anticonvulsant, antifungal, antimalarial, anticancer properties, which make them interesting for the pharmaceutical industry (Ajani *et al.*, 2015).

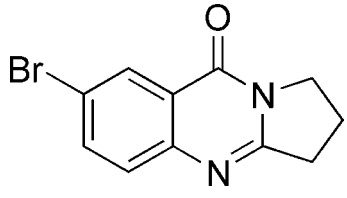

In this context, synthetic analogues of the tricyclic quinazoline-9-one-7-bromo-2,3-dihydropyrrolo[2,1-*b*]quinazolin-9(1*H*)-one have been synthesized, amongst them the title compound with a bromine atom in position 7. In comparison with a reported literature procedure (Shakhidoyatov, 1983), this compound is now obtained in higher yields (80–88%). For

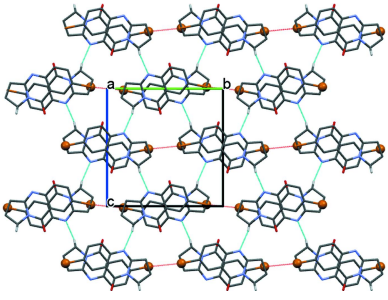

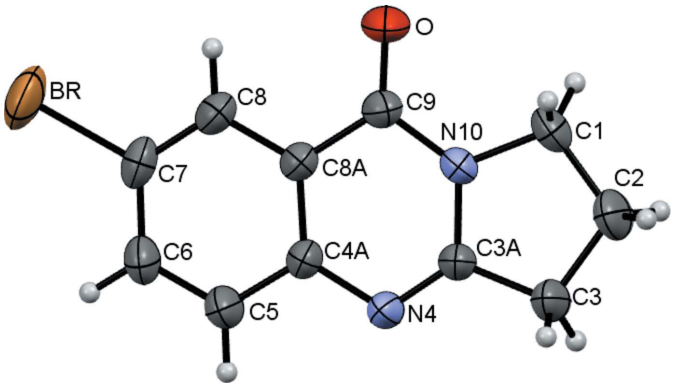

Figure 1
The molecular structure of the title compound with displacement ellipsoids drawn at the 50% probability level.

this purpose, condensation of 2-amino-5-brombenzoic acid with appropriate pyrrolidin-2-one was used whereas in the literature (Shakhidoyatov, 1983), 2-amino-5-brombenzoic acid was added to the corresponding lactam mixture with a condensing agent ($POCl_3$) at room temperature (293–298 K) and the reaction products separated by extraction after the reaction mixture was reduced to pH = 9–10 with NH_4OH. As distinguished from the reported procedure, we carried out these reactions by cooling in an ice bath at a much lower temperature (273–275 K) and for a relatively longer period of time. The reaction products were finally separated by cold NH_4OH at pH = 10–11. In general, the interactions of 7-bromo-2,3-dihydropyrrolo[2,1-*b*]quinazolin-9(1*H*)-one with aldehydes are well-studied (Abdurazakov *et al.*, 2007).

Here, we report the molecular and crystal structures as well as Hirshfeld surface analysis and the frontier molecular orbitals calculated by density functional theory (DFT) with the B3LYP functional basis set.

2. Structural commentary

The molecular structure of the title compound is shown in Fig. 1. The molecule is almost planar. In particular, the benzene and pyrimidine rings are essentially coplanar, with an r.m.s. deviations of 0.0130 Å from planarity. The remaining atoms of the dihydropyrrole ring are slightly displaced from these planes, with deviations of −0.060 (5) Å for C1, −0.154 (7) Å for flap atom C2, and 0.060 (6) Å for C3. The

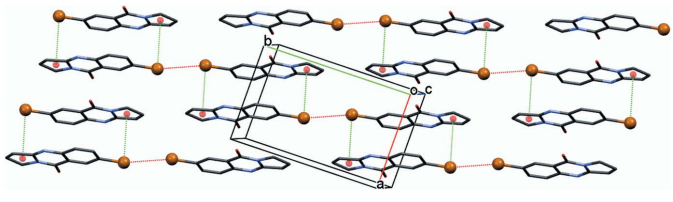

Figure 2
The packing of the title compound in a view perpendicular to (002). Intermolecular Br···Br contacts and C—Br···*Cg*1 are shown as red and green dashed lines, respectively. *Cg*1 is the centroid of the C1–C3/C3*A*/N10 ring.

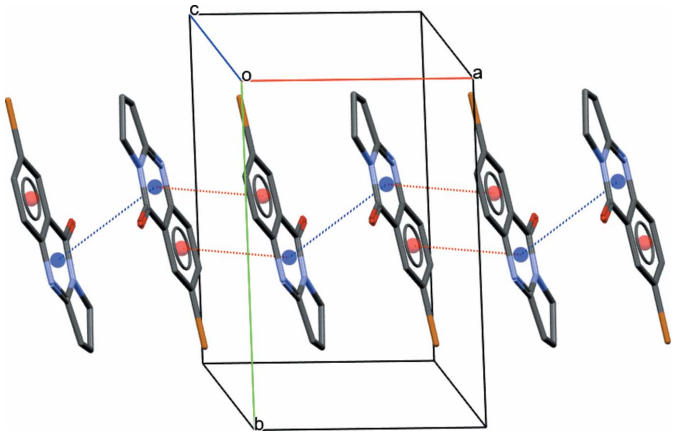

Figure 3
The packing of the title compound in a view approximately along [001], showing stacking between adjacent molecules in terms of *Cg*2···*Cg*2 (blue dashed lines) and *Cg*2···*Cg*3 (red dashed lines) interactions. *Cg*2 is the centroid (blue sphere) of the pyrimidine ring and *Cg*3 is the centroid (red sphere) of the benzene ring. H atoms are omitted for clarity.

acyclic C7—Br1 bond length 1.900 (3) Å is consistent with the data for other Br-substituted tricyclic quinazolinone derivatives (Mukarramov *et al.*, 2009; Tozhiboev *et al.*, 2007*a*; D'yakonov *et al.*, 1992; Okmanov *et al.*, 2009; Pereira *et al.*, 2005).

3. Supramolecular features

In the crystal, molecules participate in centrosymmetric halogen-bonding dimers with Br···Br intermolecular contacts of 3.5961 (5) Å, which is shorter than the sum of van der Waals radii (Bondi *et al.*, 1964) of two bromine atoms (3.66 Å). The C7—Br···Br angle amounts to 166.70 (14)°. The molecules also engage in weak C7—Br···*Cg* interactions, with Br···*Cg*1(2 − *x*, 1 − *y*, 1 − *z*) = 3.6428 (15) Å, forming a layered network (Fig. 2). Additional *π*–*π* stacking (Fig. 3) occurs between the aromatic rings of neighbouring molecules,

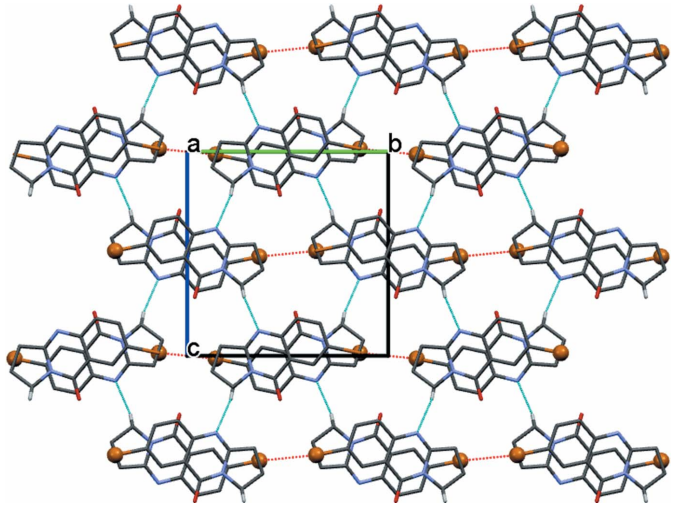

Figure 4
Packing of the title compound along [100], with intermolecular C—H···N contacts shown as light-blue dashed lines.

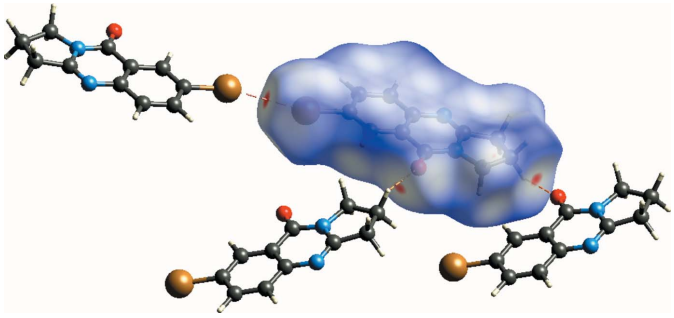

Figure 5
The Hirshfeld surface of the title compound mapped over d_{norm}, showing the close contacts.

with the distance between the centroids $Cg2\cdots Cg2^{i}$ being 3.9969 (14) Å [symmetry code: (i) $1-x, 1-y, 1-z$] and a ring slippage of 1.569 Å, and $Cg2\cdots Cg3^{ii}$ being 3.7513 (16) Å [symmetry code: (ii) $2-x, 1-y, 1-z$] and a ring slippage of 1.194 Å. Both short intermolecular contacts help to stack parallel molecules along [100]. The resulting two-dimensional network extends parallel to (002), with neighbouring layers linked through C1—H1*B*···N4 short intermolecular contacts, H1*B*···N4($x, \frac{1}{2}-y, \frac{1}{2}+z$) = 2.73 Å, C1—H1*B*···N4($x, \frac{1}{2}-y, \frac{1}{2}+z$) = 169°, to form the full three-dimensional structure (Fig. 4).

4. Hirshfeld surface analysis

In order to quantify the intermolecular interactions in the crystal of the title compound, a Hirshfeld surface (HS) analysis (Spackman *et al.*, 2009) was performed and associated two-dimensional fingerprint plots (McKinnon *et al.*, 2007) were generated with the program *CrystalExplorer* (Spackman *et al.*, 2021). The HS mapped over d_{norm} is depicted in Fig. 5, which shows the most prominent intermolecular interactions as red spots corresponding to the Br···Br, C—H···O and N—H···O contacts. The two-dimensional fingerprint plot for all contacts is given in Fig. 6*a*. H···H contacts are responsible for the largest contribution (37.2%) to the Hirshfeld surface (Fig. 6*b*). Besides these contacts, Br···H/H···Br (19.6%), O···H/H···O (11.3%), N···H/H···N (8.1%) and C···H/H···C (6.9%) interactions contribute significantly to the total Hirshfeld surface; their decomposed fingerprint plots are shown in Fig. 6*c*–*f*. The contributions of further contacts are only minor and amount to N···C/C···N (3.5%), O···C/C···O (2.0%), Br···C/C···Br (0.9%), Br···Br (0.8%), O···N/N···O (0.5%) and Br···N/N···Br (0.3%).

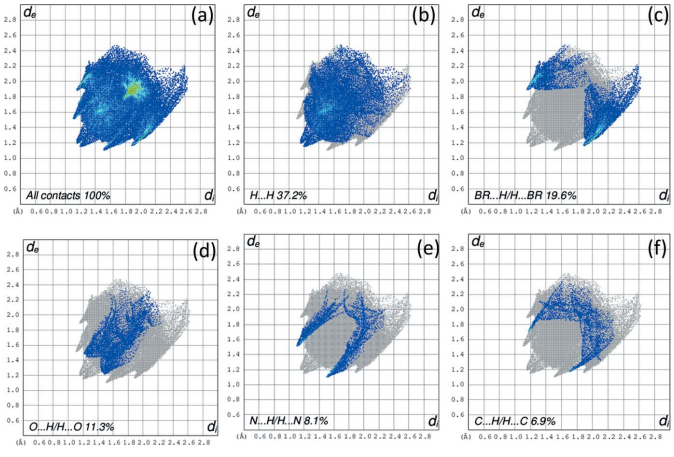

Figure 6
A view of the two-dimensional fingerprint plots for the title compound, showing (*a*) all interactions, and delineated into (*b*) H···H, (*c*) Br···H/H···Br, (*d*) O···H/H···O, (*e*) N···H/H···N and (*f*) C···H/H···C interactions. The d_i and d_e values are the closest internal and external distances (in A°) from given points on the Hirshfeld surface contacts.

5. Frontier molecular orbitals

DFT was used to calculate the frontier molecular orbitals (FMOs, Fig. 7), which give important details of how a molecule interacts with other species, for example in terms of molecular reactivity and the ability of a molecule to absorb light. From the highest occupied molecular orbital (HOMO) electrons can be donated to the lowest unoccupied molecular orbital (LUMO). Moreover, the energy of the HOMO is directly related to the ionization potential, while the LUMO energy is directly related to the electron affinity, and the resulting energy difference (or energy gap) between HOMO and LUMO gives information about the stability of a molecule. In the case where the energy gap is small, the molecule is highly polarizable and has a high chemical reactivity. By using the HOMO and LUMO energy values of a molecule, its electronegativity (c), chemical hardness (h) and chemical softness (s) can be calculated as follows: $c = (I + A)/2$; $h = (I - A)/2$; $s = 1/2h$, where I and A are the ionization potential and electron affinity, respectively, where $I = -E_{HOMO}$ and $A = -E_{LUMO}$ (Pir *et al.*, 2014; Azizov *et al.*, 2021).

E_{HOMO} and E_{LUMO}, electronegativity (c), hardness (h), potential (m), electrophilicity (w) and softness (s) for the title

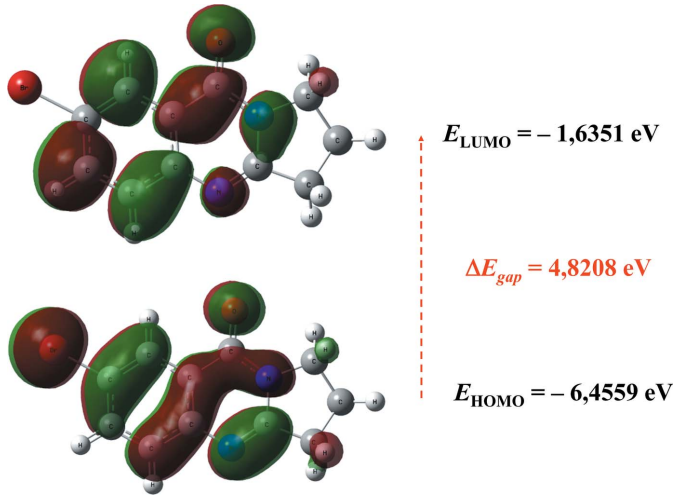

Figure 7
The frontier molecular orbitals (HOMO-LUMO) and the resulting band gap of the title molecule.

Table 1
Calculated parameters of the title molecule calculated at the B3LYP/6–311++G(d,p) level.

Parameters	DFT/B3LYP
Total energy *TE* (a.u.)	−3183.662028
E_{HOMO} (eV)	−6.4559
E_{LUMO} (eV)	−1.6351
Energy gap, ΔE (eV)	4.8208
Dipole moment, μ (Debye)	4.6478
Ionization potential, *I* (eV)	6.4559
Electron affinity, *A*	1.6351
Electronegativity, χ	4.0455
Hardness, η	2.4104
Electrophilicity index, ω	3.3949
Softness, σ	0.2074

molecule were calculated at the DFT/B3LYP level using the 6-311++G(d,p) basis set (Table 1). The values of *h* and *s* are significant for the evaluation of both reactivity and stability. The electron transition from the HOMO to the LUMO energy level is shown in Fig. 7. The energy band gap [$\Delta E = E_{LUMO} - E_{HOMO}$] of the molecule is 4.8208 eV, the frontier molecular orbital energies E_{HOMO} and E_{LUMO} being −6.4559 and −1.6351 eV, respectively. The high value of the band gap (4,8208 eV) indicates the relatively high stability of the title molecule.

6. Database survey

A search in the Cambridge Structural Database (CSD, version 2022; Groom *et al.*, 2016) gave four matches of molecules containing the 2,3-dihydropyrrolo[2,1-*b*]quinazolin-9(1*H*)-one moiety with a similar conformation to that in the title structure: deoxyvasicinone (TEFGEQ; Turgunov *et al.*, 1995), deoxyvasicinonium chloride (TEFGIU; Turgunov *et al.*, 1995), bis(deoxyvasicinonium) tetrachloridocobaltate(II) (TEFGOA; Turgunov *et al.*, 1995) and 4-oxo-2,3-tetramethylene-3,4-dihydroquinazolinium 2,3-tetramethylene-3,4-dihydroquinazol-4-one hemikis(oxalate) oxalic acid solvate (TITGUZ; Tozhiboev *et al.*, 2007*b*). A search for compounds substituted in position 7 of 2,3-dihydropyrrolo[2,1-*b*]quinazolin-9(1*H*)-one moiety gave only two hits: *N*-(9-oxo-1,2,3,9-tetrahydropyrrolo[2,1-*b*]quinazolin-7-yl)propanamide sesquihydrate (GABJAX; Elmuradov *et al.*, 2016) and 3*b*-hydroxy-7-methoxy-2,3-dihydropyrrolo[2,1-*b*]quinazolin-9(1*H*)-one monohydrate (HIHLIT; Magotra *et al.*, 1996). Comparing the listed structures with that of the title compound gave analogous complanarities of the benzene and pyrimidine rings. In the case of structures TEFGEQ, GABJAX and HIHLIT they have also similarities regarding π–π stacking interactions.

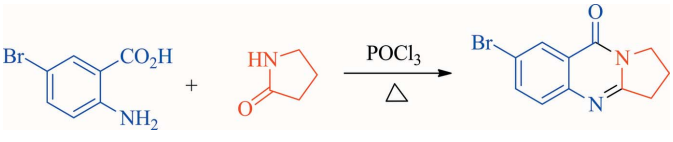

Figure 8
The reaction scheme of the title compound.

Table 2
Experimental details.

Crystal data	
Chemical formula	$C_{11}H_9BrN_2O$
M_r	265.11
Crystal system, space group	Monoclinic, $P2_1/c$
Temperature (K)	296
a, *b*, *c* (Å)	7.5654 (3), 11.4972 (2), 12.1025 (3)
β (°)	105.583 (3)
V (Å^3)	1013.99 (5)
Z	4
Radiation type	Cu *Kα*
μ (mm^{-1})	5.30
Crystal size (mm)	0.45 × 0.10 × 0.10
Data collection	
Diffractometer	XtaLAB Synergy, Single source at home/near, HyPix3000
Absorption correction	Multi-scan (*CrysAlis PRO*; Rigaku OD, 2020)
T_{min}, T_{max}	0.400, 1.000
No. of measured, independent and observed [$I > 2\sigma(I)$] reflections	9036, 1959, 1770
R_{int}	0.035
(sin $\theta/\lambda)_{max}$ (Å^{-1})	0.615
Refinement	
$R[F^2 > 2\sigma(F^2)]$, $wR(F^2)$, *S*	0.036, 0.099, 1.08
No. of reflections	1959
No. of parameters	137
H-atom treatment	H-atom parameters constrained
$\Delta\rho_{max}$, $\Delta\rho_{min}$ (e Å^{-3})	0.61, −0.56

Computer programs: *CrysAlis PRO* (Rigaku OD, 2020), *SHELXS* (Sheldrick, 2008), *SHELXL* (Sheldrick, 2015), *PLATON* (Spek, 2020) and *publCIF* (Westrip, 2010).

7. Synthesis and crystallization

The reaction scheme to yield the title compound is shown in Fig. 8. To a mixture of 4.32 g (20 mmol) 2-amino-5-bromobenzoic acid and 2.72 g (32 mmol) pyrrolidin-2-one, 21.8 g (13 ml) (d = 1.675) (0.142 mol) of phosphoroxychloride were added dropwise over 1 h at 273–275 K. The reaction mixture was then heated at 368–371 K for 2 h, it was subsequently cooled and finally poured over ice. The temperature of the mixture was kept at around 273–275 K. When the reaction mixture was completely decomposed, it was brought to pH = 10–11 with 25%$_{wt}$ ammonium hydroxide solution. The light-yellow precipitate was filtered off, dried and recrystallized from methanol. The yield of the product was 4.35 g (82%), m.p. 431–433 K (literature, m.p. = 430–431 K; Shakhidoyatov, 1983).

^{1}H NMR (400 Mz, CDCl$_3$, δ, ppm): 8.4 (1H, *d*, *J* = 2.4, H-8), 7.8 (1H, *dd*, *J* = 2.4, *J* = 8.8, H-6), 7.5 (1H, *d*, *J* = 8.8, H-5), 4.2 (2H, *q*, *J* = 7.2, H-1), 3.18 (2H, *t*, *J* = 7.6, H-3), 2.31 (2H, *m*, H-2).

8. Refinement

Crystal data, data collection and structure refinement details are summarized in Table 2. H atoms attached to C were positioned geometrically, with C—H = 0.93 Å (for aromatic) or C—H = 0.97 Å (for methylene H atoms), and were refined with U_{iso}(H) = 1.2U_{eq}(C).

Acknowledgements

The authors thank the Institute of Bioorganic Chemistry of Academy Sciences of Uzbekistan, Tashkent, Uzbekistan for providing the single-crystal XRD facility.

Funding information

Funding for this research was provided by: the Ministry of Innovative Development of Uzbekistan (grant No. F-FA-2021-408 "Study of the laws of introducing of pharmacophore fragments into the molecule on the basis of modern cross-coupling and heterocyclization reactions").

References

Abdurazakov, A. Sh., Elmuradov, B. Zh. & Shakhidoyatov, Kh. M. (2007). *Uzb. Khim. Zh.* **6**, 46–50.
Ajani, O. O., Audu, O. Y., Aderohunmu, D. V., Owolabi, F. E. & Olomieja, A. O. (2016). *Am. J. Drug Discov. Dev*, **7**, 1–24.
Ajani, O. O., Isaac, J. T., Owoeye, T. F. & Akinsiku, A. A. (2015). *Int. J. Biol. Chem.* **9**, 148–177.
Azizov, Sh., Sharipov, M., Lim, J. M., Tawfik, S. M., Kattaev, N. & Lee, Y. I. (2021). *J. Mass Spectrom.* **56**, e4611–e4620.
Bondi, A. (1964). *J. Phys. Chem.* **68**, 441–451.
D'yakonov, A. L., Telezhenetskaya, M. V. & Tashkodzhaev, B. (1992). *Chem. Nat. Compd.* **28**, 200–206.
Elmuradov, B. Zh., Shakhidoyatov, Kh. M., Drager, G. & Butenschon, H. (2016). *Eur. J. Org. Chem.* pp. 483–492.
Groom, C. R., Bruno, I. J., Lightfoot, M. P. & Ward, S. C. (2016). *Acta Cryst.* B**72**, 171–179.
Khan, I., Ibrar, A. N., Abbas, N. & Saeed, A. (2014). *Eur. J. Med. Chem.* **76**, 193–244.
Magotra, D. K., Gupta, V. K., Rajnikant, Goswami, K. N., Thappa, R. K. & Agarwal, S. G. (1996). *Acta Cryst.* C**52**, 1491–1493.
McKinnon, J. J., Jayatilaka, D. & Spackman, M. A. (2007). *Chem. Commun.* pp. 3814–3816.
Mukarramov, N. I., Okmanov, R. Ya., Utaeva, F. R., Turgunov, K. K., Tashkhodzhaev, B., Khakimova, Z. M. & Shakhidoyatov, Kh. M. (2009). *Chem. Nat. Compd.* **45**, 854–858.
Okmanov, R. Ya., Tozhiboev, A. G., Turgunov, K. K., Tashkhodzhaev, B., Mukarramov, N. I. & Shakhidoyatov, Kh. M. (2009). *J. Struct. Chem.* **50**, 382–384.
Pereira, M. F., Picot, L., Guillon, J., Léger, J.-M., Jarry, C., Thiéry, V. & Besson, T. (2005). *Tetrahedron Lett.* **46**, 3445–3447.
Pir, H., Günay, N., Avcı, D., Tamer, Ö., Tarcan, E. & Atalay, Y. (2014). *Arab. J. Sci. Eng.* **39**, 5799–5814.
Rajput, R. & Mishra, A. P. (2012). *Int. J. Pharm. Pharm. Sci.* **4**, 66–70.
Ramesh, K., Karnakar, K. G., Satish, G., Reddy, K. H. V. & Nageswar, Y. V. D. (2012). *Tetrahedron Lett.* **53**, 6095–6099.
Raymond, E., Faivre, S. & Armand, J. P. (2000). *Drugs*, **60**, 15–23.
Rigaku OD (2020). *CrysAlis PRO*. Rigaku Oxford Diffraction, Yarnton, England.
Shakhidoyatov, Kh. M. (1983). Doctoral Dissertation, University of Moscow, Russia, p. 124.
Sheldrick, G. M. (2008). *Acta Cryst.* A**64**, 112–122.
Sheldrick, G. M. (2015). *Acta Cryst.* A**71**, 3–8.
Sordella, R., Bell, D. W., Haber, D. A. & Settleman, J. (2004). *Science*, **305**, 1163–1167.
Spackman, M. A. & Jayatilaka, D. (2009). *CrystEngComm*, **11**, 19–32.
Spackman, P. R., Turner, M. J., McKinnon, J. J., Wolff, S. K., Grimwood, D. J., Jayatilaka, D. & Spackman, M. A. (2021). *J. Appl. Cryst.* **54**, 1006–1011.
Spek, A. L. (2020). *Acta Cryst.* E**76**, 1–11.
Tozhiboev, A. G., Tashkhodzhaev, B., Turgunov, K. K., Mukarramov, N. I. & Shakhidoyatov, Kh. M. (2007*a*). *J. Struct. Chem.* **48**, 534–539.
Tozhiboev, A. G., Turgunov, K. K., Tashkhodzhaev, B. & Shakhidoyatov, Kh. M. (2007*b*). *Chem. Nat. Compd.* **43**, 184–189.
Turgunov, K. K., Tashkhodzhaev, B., Molchanov, L. V. & Aripov, K. N. (1995). *Chem. Nat. Compd.* **31**, 714–718.
Westrip, S. P. (2010). *J. Appl. Cryst.* **43**, 920–925.

supporting information

Acta Cryst. (2022). E**78**, 885-889 [https://doi.org/10.1107/S2056989022007800]

Crystal structure, Hirshfeld surface analysis and DFT calculations of 7-bromo-2,3-dihydropyrrolo[2,1-*b*]quinazolin-9(1*H*)-one

Akmaljon Tojiboev, Burkhon Elmuradov, Nuritdin Kattaev, Asqar Abdurazakov, Azizbek Nasrullayev and Bakhodir Tashkhodjaev

Computing details

Data collection: *CrysAlis PRO* (Rigaku OD, 2020); cell refinement: *CrysAlis PRO* (Rigaku OD, 2020); data reduction: *CrysAlis PRO* (Rigaku OD, 2020); program(s) used to solve structure: *SHELXS* (Sheldrick, 2008); program(s) used to refine structure: *SHELXL* (Sheldrick, 2015); molecular graphics: *PLATON* (Spek, 2020); software used to prepare material for publication: *publCIF* (Westrip, 2010).

7-Bromo-2,3-dihydropyrrolo[2,1-*b*]quinazolin-9(1*H*)-one

Crystal data

$C_{11}H_9BrN_2O$
$M_r = 265.11$
Monoclinic, $P2_1/c$
$a = 7.5654$ (3) Å
$b = 11.4972$ (2) Å
$c = 12.1025$ (3) Å
$\beta = 105.583$ (3)°
$V = 1013.99$ (5) Å^3
$Z = 4$
$F(000) = 528$
$D_x = 1.737$ Mg m^{-3}
Cu $K\alpha$ radiation, $\lambda = 1.54184$ Å
Cell parameters from 5905 reflections
$\theta = 3.8$–71.3°
$\mu = 5.30$ mm^{-1}
$T = 296$ K
Prismatic, colourless
0.45 × 0.10 × 0.10 mm

Data collection

XtaLAB Synergy, Single source at home/near, HyPix3000 diffractometer
Radiation source: micro-focus sealed X-ray tube
Detector resolution: 10.0000 pixels mm^{-1}
ω scans
Absorption correction: multi-scan (*CrysAlisPro*; Rigaku OD, 2020)
$T_{min} = 0.400$, $T_{max} = 1.000$
9036 measured reflections
1959 independent reflections
1770 reflections with $I > 2\sigma(I)$
$R_{int} = 0.035$
$\theta_{max} = 71.5°$, $\theta_{min} = 5.4°$
$h = -9\rightarrow9$
$k = -14\rightarrow13$
$l = -14\rightarrow14$

Refinement

Refinement on F^2
Least-squares matrix: full
$R[F^2 > 2\sigma(F^2)] = 0.036$
$wR(F^2) = 0.099$
$S = 1.08$
1959 reflections
137 parameters
0 restraints
Hydrogen site location: inferred from neighbouring sites
H-atom parameters constrained
$w = 1/[\sigma^2(F_o^2) + (0.0459P)^2 + 0.6636P]$ where $P = (F_o^2 + 2F_c^2)/3$
$(\Delta/\sigma)_{max} = 0.005$

$\Delta\rho_{max}$ = 0.61 e Å^{-3}
$\Delta\rho_{min}$ = −0.56 e Å^{-3}

Extinction correction: SHELXL-2018/3 (Sheldrick 2015), $Fc^*=kFc[1+0.001xFc^2\lambda^3/\sin(2\theta)]^{-1/4}$
Extinction coefficient: 0.0045 (4)

Special details

Geometry. All esds (except the esd in the dihedral angle between two l.s. planes) are estimated using the full covariance matrix. The cell esds are taken into account individually in the estimation of esds in distances, angles and torsion angles; correlations between esds in cell parameters are only used when they are defined by crystal symmetry. An approximate (isotropic) treatment of cell esds is used for estimating esds involving l.s. planes.

Fractional atomic coordinates and isotropic or equivalent isotropic displacement parameters (Å^2)

	x	*y*	*z*	U_{iso}*/U_{eq}
Br	0.90737 (5)	0.85845 (3)	0.51410 (4)	0.0772 (2)
O	0.6024 (3)	0.46212 (19)	0.28785 (15)	0.0704 (6)
C1	0.5525 (4)	0.2291 (2)	0.3474 (2)	0.0524 (6)
H1A	0.615715	0.217862	0.288281	0.063*
H1B	0.424182	0.245293	0.311148	0.063*
C2	0.5725 (5)	0.1238 (3)	0.4234 (3)	0.0646 (8)
H2A	0.660804	0.070068	0.406688	0.077*
H2B	0.455714	0.084094	0.411100	0.077*
C3	0.6385 (5)	0.1665 (2)	0.5467 (2)	0.0573 (7)
H3A	0.541287	0.160567	0.584874	0.069*
H3B	0.742854	0.121317	0.589288	0.069*
C3A	0.6916 (4)	0.2907 (2)	0.53807 (19)	0.0428 (5)
N4	0.7726 (4)	0.35675 (17)	0.62262 (17)	0.0503 (5)
C4A	0.8027 (3)	0.4710 (2)	0.59434 (19)	0.0424 (5)
C5	0.8937 (4)	0.5471 (2)	0.6820 (2)	0.0569 (7)
H5	0.932797	0.519968	0.757050	0.068*
C6	0.9258 (4)	0.6610 (2)	0.6588 (2)	0.0554 (7)
H6	0.986151	0.710837	0.717397	0.066*
C7	0.8667 (4)	0.7005 (2)	0.5464 (2)	0.0490 (6)
C8	0.7793 (4)	0.6286 (2)	0.4582 (2)	0.0486 (6)
H8	0.742035	0.656476	0.383367	0.058*
C8A	0.7471 (3)	0.5135 (2)	0.48227 (19)	0.0403 (5)
C9	0.6560 (3)	0.4355 (2)	0.38867 (19)	0.0451 (5)
N10	0.6368 (3)	0.32406 (18)	0.42522 (15)	0.0405 (4)

Atomic displacement parameters (Å^2)

	U^{11}	U^{22}	U^{33}	U^{12}	U^{13}	U^{23}
Br	0.0940 (3)	0.0341 (2)	0.1020 (4)	−0.00671 (14)	0.0235 (2)	0.00799 (14)
O	0.1104 (17)	0.0553 (12)	0.0345 (9)	0.0020 (11)	0.0007 (10)	0.0064 (8)
C1	0.0651 (16)	0.0489 (15)	0.0402 (12)	−0.0045 (12)	0.0089 (11)	−0.0130 (11)
C2	0.090 (2)	0.0478 (16)	0.0519 (16)	−0.0179 (15)	0.0121 (15)	−0.0119 (12)
C3	0.088 (2)	0.0401 (13)	0.0432 (13)	−0.0170 (13)	0.0171 (13)	−0.0026 (11)
C3A	0.0572 (14)	0.0365 (12)	0.0347 (11)	−0.0038 (10)	0.0121 (10)	0.0004 (9)
N4	0.0768 (15)	0.0375 (12)	0.0338 (10)	−0.0096 (9)	0.0099 (10)	−0.0008 (8)

C4A	0.0548 (13)	0.0338 (12)	0.0377 (11)	−0.0018 (10)	0.0110 (10)	0.0000 (9)
C5	0.0807 (19)	0.0420 (14)	0.0412 (12)	−0.0082 (13)	0.0047 (12)	−0.0026 (11)
C6	0.0657 (16)	0.0411 (13)	0.0557 (15)	−0.0073 (12)	0.0100 (13)	−0.0097 (11)
C7	0.0530 (14)	0.0315 (12)	0.0638 (15)	0.0004 (10)	0.0177 (12)	0.0019 (11)
C8	0.0595 (15)	0.0385 (13)	0.0476 (13)	0.0059 (10)	0.0142 (11)	0.0086 (10)
C8A	0.0473 (12)	0.0363 (12)	0.0375 (11)	0.0042 (9)	0.0116 (9)	0.0011 (9)
C9	0.0571 (14)	0.0407 (13)	0.0354 (11)	0.0060 (10)	0.0090 (10)	0.0027 (9)
N10	0.0515 (11)	0.0373 (10)	0.0317 (9)	−0.0017 (8)	0.0093 (8)	−0.0033 (8)

Geometric parameters (Å, º)

Br—C7	1.900 (3)	C3A—N10	1.371 (3)
O—C9	1.217 (3)	N4—C4A	1.392 (3)
C1—N10	1.471 (3)	C4A—C8A	1.396 (3)
C1—C2	1.503 (4)	C4A—C5	1.404 (3)
C1—H1A	0.9700	C5—C6	1.375 (4)
C1—H1B	0.9700	C5—H5	0.9300
C2—C3	1.522 (4)	C6—C7	1.389 (4)
C2—H2A	0.9700	C6—H6	0.9300
C2—H2B	0.9700	C7—C8	1.371 (4)
C3—C3A	1.494 (4)	C8—C8A	1.391 (3)
C3—H3A	0.9700	C8—H8	0.9300
C3—H3B	0.9700	C8A—C9	1.464 (3)
C3A—N4	1.290 (3)	C9—N10	1.376 (3)
N10—C1—C2	104.5 (2)	N4—C4A—C5	118.8 (2)
N10—C1—H1A	110.8	C8A—C4A—C5	118.3 (2)
C2—C1—H1A	110.8	C6—C5—C4A	121.1 (2)
N10—C1—H1B	110.8	C6—C5—H5	119.4
C2—C1—H1B	110.8	C4A—C5—H5	119.4
H1A—C1—H1B	108.9	C5—C6—C7	118.9 (2)
C1—C2—C3	107.0 (2)	C5—C6—H6	120.6
C1—C2—H2A	110.3	C7—C6—H6	120.6
C3—C2—H2A	110.3	C8—C7—C6	121.8 (2)
C1—C2—H2B	110.3	C8—C7—Br	119.1 (2)
C3—C2—H2B	110.3	C6—C7—Br	119.1 (2)
H2A—C2—H2B	108.6	C7—C8—C8A	119.0 (2)
C3A—C3—C2	105.3 (2)	C7—C8—H8	120.5
C3A—C3—H3A	110.7	C8A—C8—H8	120.5
C2—C3—H3A	110.7	C8—C8A—C4A	120.8 (2)
C3A—C3—H3B	110.7	C8—C8A—C9	119.6 (2)
C2—C3—H3B	110.7	C4A—C8A—C9	119.6 (2)
H3A—C3—H3B	108.8	O—C9—N10	121.4 (2)
N4—C3A—N10	125.3 (2)	O—C9—C8A	125.6 (2)
N4—C3A—C3	125.9 (2)	N10—C9—C8A	112.97 (19)
N10—C3A—C3	108.8 (2)	C3A—N10—C9	123.4 (2)
C3A—N4—C4A	115.8 (2)	C3A—N10—C1	113.1 (2)
N4—C4A—C8A	122.9 (2)	C9—N10—C1	123.41 (19)

N10—C1—C2—C3	9.8 (4)	C5—C4A—C8A—C8	−0.7 (4)
C1—C2—C3—C3A	−11.4 (4)	N4—C4A—C8A—C9	−1.2 (4)
C2—C3—C3A—N4	−172.4 (3)	C5—C4A—C8A—C9	178.5 (2)
C2—C3—C3A—N10	8.8 (3)	C8—C8A—C9—O	−0.4 (4)
N10—C3A—N4—C4A	0.9 (4)	C4A—C8A—C9—O	−179.6 (3)
C3—C3A—N4—C4A	−177.8 (3)	C8—C8A—C9—N10	178.8 (2)
C3A—N4—C4A—C8A	1.0 (4)	C4A—C8A—C9—N10	−0.3 (3)
C3A—N4—C4A—C5	−178.7 (3)	N4—C3A—N10—C9	−2.6 (4)
N4—C4A—C5—C6	−179.6 (3)	C3—C3A—N10—C9	176.2 (2)
C8A—C4A—C5—C6	0.7 (4)	N4—C3A—N10—C1	178.4 (3)
C4A—C5—C6—C7	0.0 (5)	C3—C3A—N10—C1	−2.7 (3)
C5—C6—C7—C8	−0.7 (4)	O—C9—N10—C3A	−178.6 (3)
C5—C6—C7—Br	179.0 (2)	C8A—C9—N10—C3A	2.1 (3)
C6—C7—C8—C8A	0.8 (4)	O—C9—N10—C1	0.3 (4)
Br—C7—C8—C8A	−179.02 (19)	C8A—C9—N10—C1	−179.0 (2)
C7—C8—C8A—C4A	−0.1 (4)	C2—C1—N10—C3A	−4.5 (3)
C7—C8—C8A—C9	−179.2 (2)	C2—C1—N10—C9	176.5 (2)
N4—C4A—C8A—C8	179.6 (2)		